AIP | Applied Physics Letters

Plasmonic backscattering enhanced inverted photovoltaics

D. M. N. M. Dissanayake, B. Roberts, and P.-C. Ku

Citation: Appl. Phys. Lett. **99**, 113306 (2011); doi: 10.1063/1.3640217
View online: http://dx.doi.org/10.1063/1.3640217
View Table of Contents: http://apl.aip.org/resource/1/APPLAB/v99/i11
Published by the AIP Publishing LLC.

Additional information on Appl. Phys. Lett.

Journal Homepage: http://apl.aip.org/
Journal Information: http://apl.aip.org/about/about_the_journal
Top downloads: http://apl.aip.org/features/most_downloaded
Information for Authors: http://apl.aip.org/authors

ADVERTISEMENT

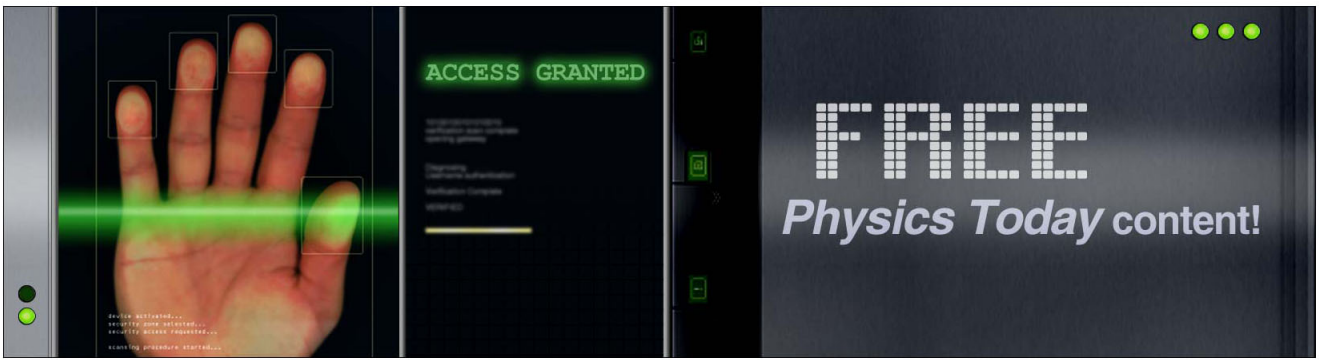

Downloaded 28 Jun 2013 to 141.211.173.82. This article is copyrighted as indicated in the abstract. Reuse of AIP content is subject to the terms at: http://apl.aip.org/about/rights_and_permissions

Plasmonic backscattering enhanced inverted photovoltaics

D. M. N. M. Dissanayake, B. Roberts, and P.-C. Ku[a)]
Department of Electrical Engineering and Computer Science, University of Michigan, Ann Arbor, Michigan 48109, USA

(Received 15 July 2011; accepted 27 August 2011; published online 16 September 2011)

A plasmonic nanoparticle incorporated inverted organic photovoltaic structure was demonstrated where a monolayer of Ag nanoparticles acted as a wavelength selective reflector. Enhanced light harvesting via plasmonic backscattering into the photovoltaic absorber was observed, resulting in a two-fold improvement in the photocurrent and increased open-circuit voltage. Further, utilizing an optical spacer, the plasmonic backscattering was spectrally controlled, thereby modulating the external quantum efficiency and the photocurrent. Unlike a regular thin-film metallic back reflector, excellent off-resonance optical transmission in excess of 80% was observed from the Ag nanoparticles, making this structure highly suitable for semi-transparent and multi-junction photovoltaic applications. © *2011 American Institute of Physics*. [doi:10.1063/1.3640217]

For solar electricity to compete favorably with fossil fuels, one must increase the power conversion efficiency while reducing the cost. Thin-film photovoltaics (PVs) such as organic polymer and amorphous silicon PVs can significantly reduce the manufacturing and materials costs.[1–3] However, in order to compensate for their poor charge transport, the absorber thickness in these PV structures is limited to few hundred nanometers, resulting in incomplete light harvesting and subsequently lower power conversion efficiency.[4,5] Although a simple metal back-reflector can easily alleviate the above trade off, the wavelength insensitivity may limit other potential benefits such as semi-transparency and being used in multi-junction PVs. Capturing light by resonant coupling to plasmonic as well as other nanoscale, light trapping structures are alternative approaches that have attracted recent interests.[6,7] Plasmonic structures consisting of metallic nanoparticles (MNPs) can be processed easily and indeed have been shown to increase the external quantum efficiency (EQE) of thin-film PVs.[7–9] However, in most studies to date, these plasmonic structures have been placed "inside" the optical or/and electrical paths of a PV device. Hence, the additional metal absorption or/and the reduced open-circuit voltage as a result of non-radiative recombination around the MNPs can negate the improvement gained by increased light capture by plasmonic structures. In this paper, we aim to show that placing plasmonic structures "outside" the optical and electrical paths of a PV device not only leads to enhanced conversion efficiency but can be used as a wavelength selective filter for semitransparent PVs and a light trapping structure for multi-junction thin-film PVs.

As a proof of concept, we placed a Ag MNP monolayer underneath an inverted organic PV device as shown in Figure 1(a), physically separating the plasmonic layer from the active region. The whole device was fabricated bottom up, starting from creating an ordered pattern of Ag nanoparticles on glass substrates (1-mm thick) using nanosphere lithography.[10] Polystyrene particles (200 nm in diameter), functionalized with carboxylic acid ligands, were spin-coated at 3500 rpm for 40 s to get a monolayer covering c.a. 1-cm^2 area (inset Fig. 1(a)), which was then used as a mask to evaporate 20 nm of Ag. The subsequent lift off of Ag by ultrasonication formed an ordered array of 45-nm wide and 20-nm high particles separated by 200 nm as shown in Fig. 1(a). Afterwards, the Ag nanoparticles were encapsulated in a ZnO layer for planarization with a varying thickness from 80 to 360 nm which also functions as an optical spacer. An Al_2O_3 layer (15-nm thick) was deposited on top of the ZnO by atomic layer deposition as an

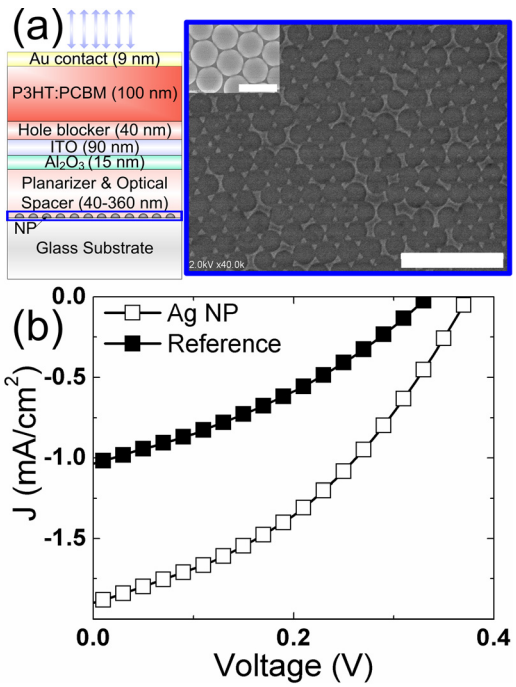

FIG. 1. (Color online) (a) Schematic of the inverted organic-polymer PV fabricated with Ag MNPs placed outside the photoactive region. Device is illuminated from the Au semitransparent contact. A bird's-eye view of the Ag MNPs measured by SEM is shown (scale bar is 1 μm). The inset shows an SEM image of a monolayer of 200-nm diameter polystyrene particles used for nanosphere lithography (scale bar is 300 nm). (b) Current-density voltage (J-V) characteristics under AM1.5 illumination of the inverted PV with Ag metal nanoparticles (white squares) with 80-nm optical spacer and a reference inverted PV (black squares).

[a)]Author to whom correspondence should be addressed. Electronic mail: peicheng@umich.edu.

 © 2011 American Institute of Physics

Downloaded 28 Jun 2013 to 141.211.173.82. This article is copyrighted as indicated in the abstract. Reuse of AIP content is subject to the terms at: http://apl.aip.org/about/rights_and_permissions

insulator between the plasmonic layer and the top PV. Following this, an indium tin oxide (ITO) (40 Ω/sq measured resistivity) layer was deposited (90-nm thick) as the bottom transparent contact and was coated by a hole-blocking layer of ZnO (40-nm thick).[11] The active layer was formed by a spin coated (700 rpm for 20 s) 12 mg/ml solution of poly-3-helythiophene and phenyl-C61-butyric acid methyl ester (PCBM) (1:0.8) in dichlorobenzene. Finally, a 9-nm thick Au was deposited by e-beam evaporation on the organic layer as the semi-transparent top electrode.

This inverted PV is illuminated through the thin Au top layer and the photocarriers generated within the active layer are collected as electrons from ITO, via a hole blocking layer, and holes from the high work-function Au electrode. Fig. 1(b) shows the current density vs. voltage plot of the inverted PV with MNP (empty-squares) and a reference inverted PV without the Ag MNPs (black squares), under AM1.5 illumination. The inverted Ag MNP PV shows higher short circuit current (J_{sc}) (1.9 mA/cm^2) than the reference (1.03 mA/cm^2). This nearly two-fold increase in photocurrent is attributed to enhanced exciton generation by resonant backscatter of the incident light from the MNPs to the PV active layer. These results corroborate our theoretical predications of long-range plasmonic backscattering from MNP.[12] Further to the improved photocurrent, the Ag MNP inverted PV also shows a slightly higher open circuit voltage (V_{oc}) (0.37 V) compared to reference PV (0.33 V). Improvement in V_{oc} is attributed to the increased photocurrent (I_p) of the Ag MNP inverted PV, following the Shockley relation: $V_{oc} \propto \ln(I_p/I_s + 1)$ where I_s (~1 μA) is the reverse saturation current. We justify the above by taking the V_{oc} ratio between the Ag MNP based and reference inverted PVs, $V_{oc}^{MNP}/V_{oc}^{REF} = 0.37/0.33$, which is identical to the ratio between the respective photocurrent expressions: $\ln(I_P^{MNP}/I_s + 1)/\ln(I_P^{REF}/I_s + 1) = \ln(191)/\ln(104)$. Also, the overall power conversion efficiency in the Ag MNP inverted PV (0.27%) increased by a factor of 2.4 in comparison to the reference PV (0.11%). Therefore, this plasmonic device architecture is seen to improve J_{sc} and the power conversion efficiency of the inverted PV by backscattering the incident light to the absorber layer from outside the active region.

Next, we study the performance of our inverted plasmonic PV by modulating the backscattering using the optical spacer layer. Figure 2 shows the J_{sc} of the devices measured under AM1.5 with the optical spacer thickness varied from 80 to 360 nm. A periodic change in J_{sc} is observed with the optical spacer thickness. To elucidate the physics underlying the modulation of J_{sc} by the optical spacer, an EQE measurement was carried out. Figure 3 shows the EQE of three devices with optical spacer thickness 80 nm (black circles), 120 nm (red triangles), and 200 nm (blue squares) with distinct peaks, indicated by the dotted lines, at 570, 495, and 530 nm wavelengths, respectively. Since photocurrent is a multiplication of EQE with AM1.5 intensity, the shifts in EQE peaks can cause changes in photocurrent with the optical spacer thickness as observed earlier. We attribute above EQE peaks to resonant optical modes within the cavity, formed by tuning of the backscattering from the Ag MNP via an optical spacer.[12] Importantly, as shown in inset Fig. 3, irrespective

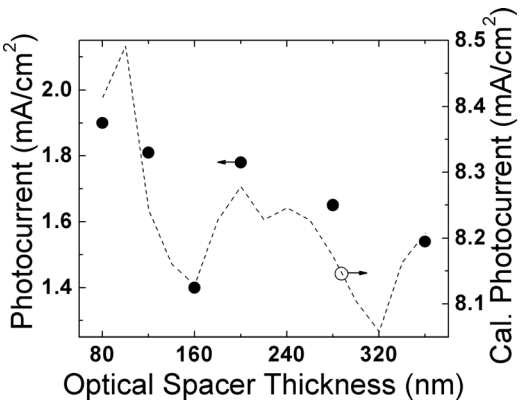

FIG. 2. Experimental (black circles) and calculated (black dashed line) photocurrent with varying optical spacer thicknesses under AM1.5 illumination.

of the spacer thickness, the Ag MNP inverted PVs (black, red, and blue circles) show higher EQE compared to a reference inverted PV without MNPs (black line) justifying the higher photocurrent observed for the Ag MNP inverted PV in Figure 1(b).

We carried out optical simulations using full-field finite differential time domain (FDTD) and transfer matrix methods to determine the optical absorption intensity within the P3HT:PCBM layer at varied optical spacer thickness.[12,13] The optical constants used in these simulations for P3HT, PCBM, Au, ITO, ZnO, Al_2O_3, and Ag were obtained through literature.[14] For FDTD simulation, a 3-dimensional Ag MNPs embedded within the material stack was considered and the objects were modeled by their complex dielectric constants $\varepsilon = \varepsilon' + i\varepsilon''$. A broad spectrum optical pulse at normal incidence was propagated through this geometry and the optical power absorbed within the P3HT:PCBM layer was found using MIT Electromagnetic Equation Propagation.[15] These FDTD calculated active layer absorption peaks, for varied optical spacers, were found to closely follow the EQE curves. However, magnitude of these absorptions did not corroborate the EQE results within the off-resonance wavelength range. We attributed this to the non-uniformity of the deposited MNPs (scanning electron microscopy (SEM) Fig.

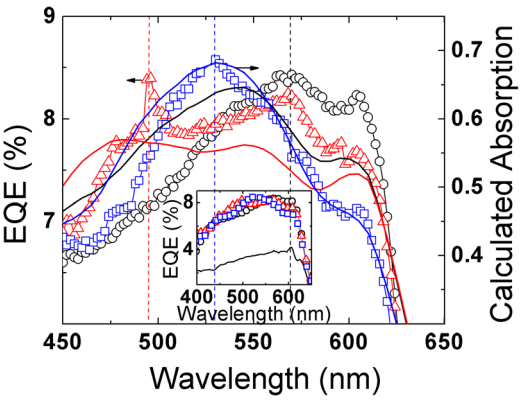

FIG. 3. (Color online) EQE of the Ag MNP based PV with optical spacer thicknesses of 80 nm (black circles), 120 nm (red triangles), and 200 nm (blue squares), respectively. Absorption in the PV absorber was calculated using a weighted average between transfer-matrix and finite difference time domain methods. The dashed lines indicate the EQE peak positions. Inset shows the EQE of the reference inverted PV without MNP (black line) together with the EQE of the Ag MNP PVs with spacer thicknesses as given above.

Downloaded 28 Jun 2013 to 141.211.173.82. This article is copyrighted as indicated in the abstract. Reuse of AIP content is subject to the terms at: http://apl.aip.org/about/rights_and_permissions

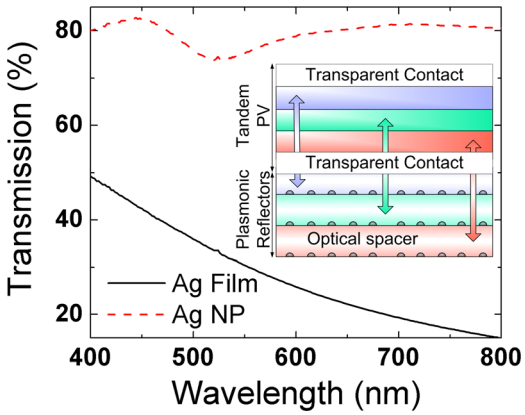

FIG. 4. (Color online) Optical transmission measurements of a monolayer of Ag MNPs (dashed line) and a 20-nm thick Ag film (solid line) carried out on 1 mm thick standard microscope glass substrates. Inset shows a schematic of a proposed plasmonic nanoparticle engineered multi-junction inverted PV with multiple plasmonic backscattering layers. The optical spacer thickness is varied to maximize light harvesting for different wavelength bands via the optical cavity effect.

1(a)). Alternatively, by taking the measured optical constants of the Ag MNPs and considering the MNP layer as an effective thin-film with comparable optical density, the absorption within P3HT:PCBM was modeled using the transfer matrix method. This approach captured the resonant scattering as well as the ensemble reflection effect of the MNPs, corroborating the absorption with the EQE measurements albeit with modest fitting to the resonance peaks.

Therefore, we used a weighted average of the P3HT:PCBM absorptions calculated from both transfer matrix and FDTD, to capture the ensemble reflection due to MNP non-uniformity using transfer matrix and the resonant backscattering from MNPs using FDTD, respectively (Fig. 3). It can be seen that the absorption peaks for 80-nm (black line), 120-nm (red line), and 200-nm (blue line) optical spacer thicknesses match approximately to the corresponding EQE peaks at the dotted lines. This clearly indicates that optical modulation of the backscattering is the direct cause of the change in the EQE. Furthermore, by considering unity internal quantum efficiency, we calculate the J_{sc} using the calculated P3HT:PCBM optical absorption for varied optical spacer thickness (black dashed line in Fig. 2). It is evident that the photocurrent generated from the plasmonic PV is modulated according to the optical spacer thickness agreeing closely with the experimental results.

In Fig. 4, the optical transmission of the Ag-MNP-coated substrate (dashed line) shows a dip at 525 nm wavelength, corresponding to the plasmon resonance of the Ag MNPs. In contrast, the off-resonance light passes through at approximately 80% transmission, which is considerably greater than a comparable 20-nm thick film of Ag (solid line). Therefore, the Ag MNPs function as a wavelength selective backscattering layer providing solar energy capture while sustaining an excellent off-resonance optical transmission which can be ideal for semitransparent PVs. Furthermore, this property allows one to stack multiple MNP backreflectors tuned to different resonance wavelengths to be used with a tandem cell structure as illustrated in the inset of Fig. 4. The enhanced backscattering can be independently tuned for each pair of absorber and the MNP layer via an optical spacer, allowing enhanced photocurrent and facilitating current matching among different junctions.[16]

In conclusion, we demonstrate an inverted PV device by using a monolayer of Ag MNP as an efficient back-reflector. The plasmonic PV delivers improved performance relative to a reference inverted PV. Furthermore, the plasmonic inverted PVs optical properties can be tuned using the optical spacer to modulate the optical intensity within the absorber region to maximize the photocurrent. Further, increase of the cell efficiency can be achieved by replacing the top metal contact with a low-loss transparent electrode.[17] Finally, we discussed the applications of the proposed plasmonic structure as a wavelength selective filter for semi-transparent PVs and a light harvesting structure in multi-junction thin-film PVs.

This work is supported as part of the Center for Solar and Thermal Energy Conversion, an Energy Frontier Research Center funded by the U.S. Department of Energy Office of Science, Office of Basic Energy Sciences under Award No. DE-SC0000957.

[1]A. G. Berger and C. Healing, Sol. Energy Mater. Sol. Cell. **62**, 1 (2000).
[2]B. Oregano and M. Gretel, Nature **353**, 737 (1991).
[3]H. Hoppe and N. S. Sarcastic, J. Mater. Res. **19**, 1924 (2004).
[4]S. R. Forrest, Mat. Res. Soc. Bull. **30**, 28 (2005).
[5]P. Pumas, A. Yakima, and S. R. Forrest, J. Appl. Phys. **93**, 3693 (2003).
[6]J. Zhu, Z. Yu, S. Fan, and Y. Cui, Mat. Sci. Eng. R **70**, 330 (2010).
[7]H. A. Atwater and A. Pullman, Nature Mater. **9**, 205 (2010).
[8]S. Pillar, K. R. Catchpole, T. Trope, and M. A. Green, J. Appl. Phys. **101**, 093105 (2007).
[9]M. Kang, T. Xat, H. Park, X. Lou, and L. Gao, Adv. Mater. **22**, 4378 (2010).
[10]J. C. Hulteen, D. A. Treichel, M. T. Smith, M. L. Duval, T. R. Jensen, and R. P. Van Duyne, J. Phys. Chem. B **103**, 3854 (1999).
[11]C. Chou, W. Kwan, Z. Hong, L. Chen, and Y. Yang, Adv. Mater. **23**, 1282 (2011).
[12]B. Roberts and P.-C. Ku, Photovoltaic Specialists Conference (PVSC), 2010 35th IEEE, pp. 002952–002954 (2010).
[13]L. A. Pettersson, L. S. Roman, and O. Inganas, J. Appl. Phys. **86**, 487 (1999).
[14]G. F. Burkhard, E. T. Hoke, and M. McGehee, Adv. Mater. **22**, 3293 (2010).
[15]A. F. Oskooi, D. Roundy, M. Ibanescu, P. Bermel, J. D. Joannopoulos, and S. G. Johnson, Comput. Phys. Commun. **181**, 687 (2010).
[16]M. A. Green, Prog. Photovoltaics **9**, 123 (2001).
[17]R. Lunt and V. Bulovic, Appl. Phys. Lett. **98**, 113305 (2011).

Downloaded 28 Jun 2013 to 141.211.173.82. This article is copyrighted as indicated in the abstract. Reuse of AIP content is subject to the terms at: http://apl.aip.org/about/rights_and_permissions